

Phonon Linewidths and Electron Phonon Coupling in Nanotubes

Michele Lazzeri^{1,*}, S. Piscanec², Francesco Mauri¹, A.C. Ferrari^{2,†} and J. Robertson²

¹*Institut de Minéralogie et de Physique des Milieux Condensés, 4 Place Jussieu, 75252, Paris cedex 05, France*

²*Department of Engineering, University of Cambridge, Cambridge CB2 1PZ, UK*

(Dated: November 26, 2024)

We prove that Electron-phonon coupling (EPC) is the major source of broadening for the Raman G and G⁻ peaks in graphite and metallic nanotubes. This allows us to directly measure the optical-phonon EPCs from the G and G⁻ linewidths. The experimental EPCs compare extremely well with those from density functional theory. We show that the EPC explains the difference in the Raman spectra of metallic and semiconducting nanotubes and their dependence on tube diameter. We dismiss the common assignment of the G⁻ peak in metallic nanotubes to a Fano resonance between phonons and plasmons. We assign the G⁺ and G⁻ peaks to TO (tangential) and LO (axial) modes.

PACS numbers: 73.63.Fg, 63.20.Kr, 73.22.-f

Electron-phonon coupling (EPC) is a key physical parameter in nanotubes. Ballistic transport, superconductivity, excited state dynamics, Raman spectra and phonon dispersions all fundamentally depend on it. In particular, the optical phonons EPC are extremely relevant since electron scattering by optical phonons sets the ultimate limit to high field ballistic transport [1, 2, 3, 4, 5]. Furthermore, they play a key role in defining the phonon dispersions [6] and the Raman spectra of metallic and semiconducting single wall nanotubes (SWNT), which show different features [7, 8, 9, 10, 11, 12, 13, 14, 15, 16, 17, 18]. Several theoretical and experimental investigations of acoustic phonons EPC have been published (see, e.g., Ref. [19]). However, only tight-binding calculations of optical phonons EPC were performed, with contrasting results [1, 2, 20, 21, 22, 23]. More crucially, no direct measurement of optical phonons EPC has been reported to validate these calculations.

In this Letter we prove that the optical phonons EPC are the major source of broadening for the Raman G and G⁻ peaks in graphite and metallic SWNTs. We show that the experimental Raman linewidths provide a direct EPC measurement. The EPC are also responsible for the the G⁺ and G⁻ splitting in metallic SWNTs. This allows us to unambiguously assign the G⁺ and G⁻ peaks to TO (tangential) and LO (axial) modes, in contrast to what often done [7, 8, 10, 11, 12, 15]. We dismiss the common assignment of the G⁻ peak in metallic SWNTs to a Fano resonance between phonons and plasmons [10, 11, 12, 13, 24, 25].

In a perfect crystal, the linewidth γ of a phonon is determined by its interaction with other elementary excitations. Usually, $\gamma = \gamma^{an} + \gamma^{EP}$, where γ^{an} is due to the interaction with other phonons and γ^{EP} with electron-hole pairs. γ^{an} is determined by anharmonic terms in the interatomic potential and is always there. γ^{EP} is determined by the EPC and is present only in systems where the electron gap is zero. If the anharmonic contribution γ^{an} is negligible or otherwise known, measuring the linewidth is the simplest way to determine the EPC.

A phonon is described by a wave vector \mathbf{q} , branch index η and frequency $\omega_{\mathbf{q}\eta}$. We consider a mean-field single particle formalism, such as density functional theory (DFT) or Hartree-Fock. The EPC contribution to $\gamma_{\mathbf{q}\eta}$ is given by the Fermi golden rule [26]:

$$\gamma_{\mathbf{q}\eta}^{EP} = \frac{4\pi}{N_{\mathbf{k}}} \sum_{\mathbf{k}, i, j} |g_{(\mathbf{k}+\mathbf{q})j, \mathbf{k}i}|^2 [f_{\mathbf{k}i} - f_{(\mathbf{k}+\mathbf{q})j}] \times \delta[\epsilon_{\mathbf{k}i} - \epsilon_{(\mathbf{k}+\mathbf{q})j} + \hbar\omega_{\mathbf{q}\eta}], \quad (1)$$

where the sum is on the electron vectors \mathbf{k} and bands i and j , $N_{\mathbf{k}}$ is the number of \mathbf{k} vectors, $f_{\mathbf{k}i}$ is the occupation of the electron state $|\mathbf{k}, i\rangle$, with energy $\epsilon_{\mathbf{k}i}$, δ is the Dirac distribution. $g_{(\mathbf{k}+\mathbf{q})j, \mathbf{k}i} = D_{(\mathbf{k}+\mathbf{q})j, \mathbf{k}i} \sqrt{\hbar/(2M\omega_{\mathbf{q}\eta})}$, where M is the atomic mass. $D_{(\mathbf{k}+\mathbf{q})j, \mathbf{k}i} = \langle \mathbf{k} + \mathbf{q}, j | \Delta V_{\mathbf{q}\eta} | \mathbf{k}, i \rangle$ and $\Delta V_{\mathbf{q}\eta}$ is the potential derivative with respect to the phonon displacement. D is the EPC.

The electron states contributing to the sum in Eq. 1 are selected by the energy conservation condition $\epsilon_{\mathbf{k}i} + \hbar\omega_{\mathbf{q}\eta} = \epsilon_{(\mathbf{k}+\mathbf{q})j}$. Also, the state $\mathbf{k}i$ has to be occupied and $(\mathbf{k} + \mathbf{q})j$ empty, so that the term $[f_{\mathbf{k}i} - f_{(\mathbf{k}+\mathbf{q})j}] \neq 0$. Thus, only electrons in the vicinity of the Fermi level contribute to γ^{EP} . In insulating and semiconducting systems $\gamma^{EP} = 0$. In general, a precise estimate of γ^{EP} from Eq. 1 is possible only after an accurate determination of the Fermi surface. However, graphite and SWNTs are very fortunate cases. Thanks to their particular band structure, γ^{EP} is given by a simple analytic formula.

In general, the EPC determines both phonon dispersions and linewidths. We first consider the case of graphite and show that both dispersion and linewidths give a direct measure of the EPC at Γ .

The electron bands of graphite are well described by those of a two dimensional graphene sheet. In graphene, the gap is zero for the π bands at the two equivalent \mathbf{K} and $\mathbf{K}' = 2\mathbf{K}$ points of the Brillouin zone. We define $\langle D_{\Gamma}^2 \rangle_F = \sum_{i,j}^{\pi} |D_{\mathbf{K}i, \mathbf{K}j}|^2 / 4$, where the sum is on the two degenerate π bands at the Fermi level ϵ_F . We consider the EPC relative to the E_{2g} phonon at Γ . The Γ -E_{2g} mode is doubly degenerate and consists of an antiphase

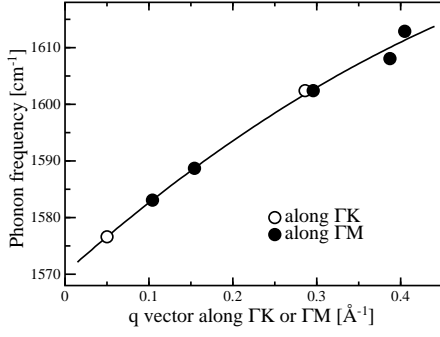


FIG. 1: Graphite phonon dispersion of the highest optical branch near Γ . Dots are inelastic X-ray measurements from Ref. [27]. The line is a quadratic fit.

in-plane motion. For a small non zero \mathbf{q} near Γ , this splits into a quasi longitudinal (LO) and quasi transverse (TO) branch, corresponding to an atomic motion parallel and perpendicular to \mathbf{q} . From DFT calculations we get $\langle D_{\Gamma}^2 \rangle_F = 45.60 (\text{eV}/\text{\AA})^2$ for both LO and TO modes [6].

We have previously shown that graphite has two Kohn anomalies in the phonon dispersions for the Γ - E_{2g} and \mathbf{K} - A'_1 modes [6]. Due to the anomaly, the dispersion near Γ of the E_{2g} -LO mode is almost linear, with slope S_{Γ}^{LO} [6]:

$$S_{\Gamma}^{\text{LO}} = \frac{\sqrt{3}\hbar a_0^2}{8M\omega_{\Gamma}\beta} \langle D_{\Gamma}^2 \rangle_F, \quad (2)$$

where $a_0 = 2.46 \text{ \AA}$ is the graphite lattice spacing, $\beta = 5.52 \text{ \AA eV}$ is the slope of the electron bands near ϵ_F , M is the carbon atomic mass and ω_{Γ} is the frequency of the E_{2g} phonon ($\hbar\omega_{\Gamma} = 196.0 \text{ meV}$). Eq. 2 shows that $\langle D_{\Gamma}^2 \rangle_F$ can be directly measured from the experimental S_{Γ}^{LO} . The phonons around Γ have been measured by several groups with close agreement. From a quadratic fit to the most recent data of ref. [27] (Fig. 1) we get $S_{\Gamma}^{\text{LO}} = 133 \text{ cm}^{-1}\text{\AA}$. From Eq. 2 we have $\langle D_{\Gamma}^2 \rangle_F = 39 (\text{eV}/\text{\AA})^2$, in good agreement with DFT.

We now show that the Full Width at Half Maximum (FWHM) of the graphite G peak gives another independent EPC measurement. The G peak of graphite is due to the Γ - E_{2g} phonon [28]. We use Eq. 1 to compute the width, $\gamma_{\Gamma}^{\text{EP}}$, for this mode. Close to \mathbf{K} , we assume the π bands dispersion to be conic from the Fermi level ϵ_F , with slope β (Fig. 2a) [29]. For both LO and TO modes:

$$\gamma_{\Gamma}^{\text{EP}} = \frac{\sqrt{3}a_0^2\hbar^2}{4M\beta^2} \langle D_{\Gamma}^2 \rangle_F. \quad (3)$$

We then measure FWHM(G) for a single-crystal graphite similar to that of Ref. [27]. Its Raman spectrum does not show any D peak (Reich in [15] and [30]), thus we exclude extra broadening due to disorder [31]. By fitting the G peak with a Lorentzian we get $\text{FWHM(G)} = 13 \text{ cm}^{-1}$. Temperature dependent measurements show no increase of FWHM(G) in the 2K-900K range [30]. Our Raman

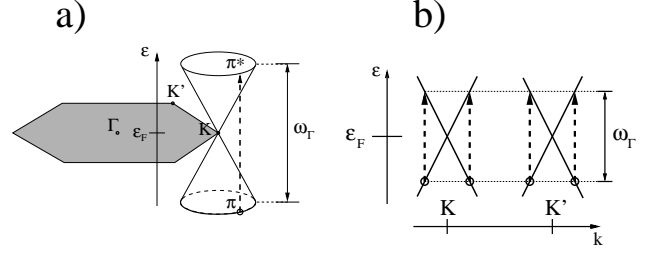


FIG. 2: Electron bands around \mathbf{K} in graphene (a) and in a metallic tube (b). Shaded area is the graphene Brillouin zone. Dashed arrows: decay processes for a Γ phonon.

spectrometer resolution is $\sim 1.5 \text{ cm}^{-1}$ [30]. We thus assume an anharmonic contribution lower than the spectral resolution $\gamma_G^{\text{an}} < 1.5 \text{ cm}^{-1}$. Thus, we estimate $\gamma_{\Gamma}^{\text{EP}} \sim 11.5 \text{ cm}^{-1}$. Then, from Eq. 3, $\langle D_{\Gamma}^2 \rangle_F \sim 47 (\text{eV}/\text{\AA})^2$. This compares very well with DFT, again confirming that γ_G^{an} is small.

Finally, near Γ the conservation of the energy and momentum in Eq. 1, implies:

$$\gamma_{\mathbf{q}}^{\text{EP}} = 0 \Leftrightarrow q \geq \hbar\omega_{\Gamma}/\beta. \quad (4)$$

This condition is satisfied by the E_{2g} phonon, involved in the Raman G peak of graphite. On the other hand, the double resonant mode close to Γ , which gives the D' peak at $\sim 1615 \text{ cm}^{-1}$, does not satisfy it. D' is indeed sharper than the G peak [32].

In summary, we presented two independent measurements of the graphite Γ - E_{2g} EPC. These are consistent with each other and with DFT. We now consider SWNTs.

The G peak of SWNTs can be fit with only two components, G^+ and G^- [11]. Semiconducting SWNTs have sharp G^+ and G^- , whilst metallic SWNTs have a broad downshifted G^- [7, 8, 9, 10, 11, 12, 13, 14, 15, 16, 17, 18]. The G^- band shows a strong diameter dependence, being lower in frequency for smaller diameters [11]. This suggested its attribution to a tangential mode, whose circumferential atoms displacements would be most affected by a variation in diameter [10]. Thus, the G^+ and G^- peaks are often assigned to LO (axial) and TO (tangential) modes [7, 8, 10, 11, 12, 15].

Conflicting reports exist on the presence and relative intensity of the G^- band in isolated versus bundled metallic tubes. It has been claimed that this peak is as intense in isolated SWNTs as in bundles [11, 17, 18]; that it is smaller [12, 14, 16]; or that it can be absent [24]. The G^- peak is also thought to represent a Fano resonance due to phonon coupling with plasmons [10, 12, 13, 24, 25]. Such phonon-plasmon coupling would either need [13] or not need [10, 25] a finite phonon wavevector for its activation. The theory of Refs. [10, 25] predicts the phonon-plasmon peak to be intrinsic in single SWNT, in contrast with [24]. On the other hand, the theory in

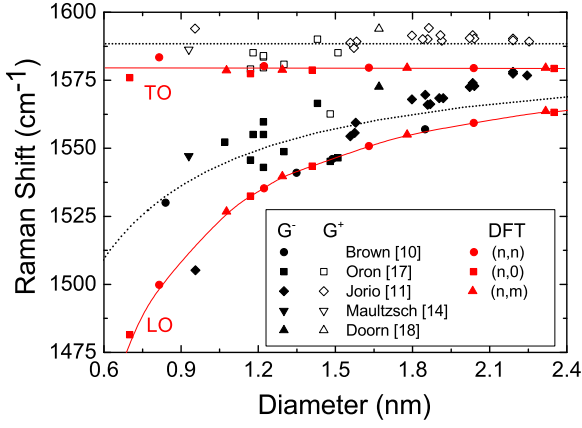


FIG. 3: (color online) Black points: experimental G^+ and G^- in metallic SWNTs vs. diameter. Red points: DFT for armchair [from (3,3) to (18,18)], zigzag [from (9,0) to (30,0)] and chiral tubes [(5,2), (12,3), (16,1), (16,10), (20,14)]. Lines: fit of Eq. 5 to the experimental and DFT data.

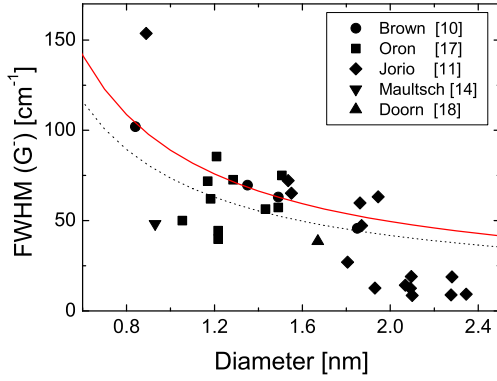


FIG. 4: Experimental FWHM(G^-) in metallic SWNTs vs. diameter. Solid line: DFT. Dotted line: fit of $\text{FWHM} = \gamma_{\Gamma-LO}^{EP} + \gamma^{an}$, with $\gamma_{\Gamma-LO}^{EP}$ from Eq. 6 and $\gamma^{an} = 10 \text{ cm}^{-1}$.

Ref. [13] requires several tubes (>20) in a bundle in order to observe a significant G^- intensity, in contrast with the experimental observation that bundles with very few metallic tubes show a significant G^- [14, 16, 17, 18, 24]. Ref. [13] also predicts a G^- upshift with number of tubes in the bundle, in contrast with Ref. [24], which shows a downshift, and with Refs. [10, 11, 17], which show that the G^- position depends on the tube diameter and not bundle size. Finally, the G^- position predicted by [13, 25] is at least 200 cm^{-1} lower than that measured [7, 8, 9, 10, 11, 12, 14, 15, 16, 17, 18]. Thus, all the proposed theories for phonon-plasmon coupling [10, 13, 25] are very qualitative, require the guess of several physical quantities, and fail to predict in a precise, quantitative, parameter-free way the observed line-shapes and their dependence on the SWNT diameter.

We now show that, like in graphite, the EPC *per se* gives the main contribution to the G^- position and FWHM, even in the absence of phonon-plasmon cou-

pling. Surprisingly, this has not been considered so far. However, it is clear that, if phonons do not couple to electrons, they certainly cannot couple to plasmons.

We compute the phonon frequencies for several metallic SWNTs using DFT (details are in Refs. [3, 33]). For all metallic tubes, of *any chirality*, we get a splitting of the modes corresponding to the graphite Γ - E_{2g} into quasi transverse (TO) and a quasi longitudinal (LO), corresponding to an atomic motion tangential to the SWNT axis or parallel to it. The LO frequency is *smaller* than the TO and has a strong diameter dependence (Fig. 3). This is the opposite of what originally proposed, i.e. that a tangential mode should have a much stronger diameter dependence than an axial one [7, 8, 10, 11, 12, 15]. This counter-intuitive result can be understood only considering the presence of a Kohn anomaly in the phonon dispersion of metallic SWNTs [6, 33, 34]. The Kohn anomaly lowers the frequency of phonons having a significant EPC. While the LO EPC is large, the TO EPC is zero. Thus, the LO frequency is smaller than the TO. Furthermore, from the dependence of the EPC on the tube diameter d [3], we get the analytic result [33]:

$$\omega_{LO}^2 = \omega_{TO}^2 - C_M/d \quad (5)$$

with C_M a constant. We thus assign the G^- peak to the LO (axial) mode and the G^+ to the TO (tangential) mode. Fig. 3 compares our DFT calculations with experiments. The agreement is excellent, considering that no fitting parameters are used. If we fit Eq. 5 to Fig. 3, we get $C_M = 1.52 \times 10^5 \text{ cm}^{-2} \text{ nm}$; $\omega_{TO} = 1591 \text{ cm}^{-1}$. Note that a $1/d^4$ dependence of $\omega_{G^-}^2$ was previously suggested based on phonon-plasmon coupling [10, 11].

Now we use Eq. 1 to derive the EPC contribution to FWHM(G^+) and FWHM(G^-) in metallic SWNTs. The EPC of a SWNT can be obtained from the graphite EPC $\langle D_{\Gamma}^2 \rangle_F$ via zone-folding (valid for $d \geq 0.8 \text{ nm}$, i.e. for the vast majority of SWNTs used in experiments and devices) [3]. Four scattering processes are involved (Fig. 2-b) and the LO and TO linewidths are:

$$\gamma_{\Gamma-LO}^{EP} = \frac{2\sqrt{3}\hbar a_0^2}{\pi M \omega_{\Gamma} \beta} \frac{\langle D_{\Gamma}^2 \rangle_F}{d}; \quad \gamma_{\Gamma-TO}^{EP} = 0. \quad (6)$$

Eq. 6 is a key result. It shows that the EPC contributes to the linewidth only for the LO mode in metallic SWNTs. For semiconducting SWNTs the EPC contribution is zero for both the TO and LO modes, since the gap does not allow to satisfy the energy conservation in Eq. 1.

This confirms our assignment of the G^- and G^+ Raman peaks to the LO and TO modes. Experimentally, in semiconducting SWNTs FWHM(G^+) and FWHM(G^-) are similar (both are $\simeq 10 \text{ cm}^{-1}$), while in metallic tubes FWHM(G^-) $\simeq 60 \text{ cm}^{-1}$ and FWHM(G^+) $\simeq 10 \text{ cm}^{-1}$, for a given d [11, 17]. The large FWHM(G^-) in metallic SWNTs is due the large γ^{EP} and the small FWHM(G^+) is entirely anharmonic in origin [35]. Thus, even if

FWHM(G) in graphite and FWHM(G⁺) in SWNTs are similar, their origin is totally different. This also explains why a FWHM(G⁺) < FWHM(G) can be seen [11].

Eq. 6 explains the 1/d dependence of FWHM(G⁻) in metallic SWNTs [11]. Then, using Eq. 6, $\langle D_{\Gamma}^2 \rangle_F$ can be directly fit from the experimental FWHM(G⁻) (Fig. 4). We find $\langle D_{\Gamma}^2 \rangle_F = 37(\text{eV}/\text{\AA})^2$, again in agreement with DFT. Note that, while the DFT $\langle D_{\Gamma}^2 \rangle_F$ is that of planar graphene, the fitted $\langle D_{\Gamma}^2 \rangle_F$ is obtained from measurements of SWNTs. Thus, the good agreement between the two values is a direct verification that the SWNT EPC can be obtained by folding the graphene EPC [3].

The most common process involved in Raman scattering is single resonance. Double resonance is necessary to explain the activation of otherwise inactive phonons away from Γ , such as the D peak [14, 37]. It has been suggested that even the G⁺ and G⁻ peaks in SWNTs are always double resonant [15, 36]. However, if the laser excitation energy satisfies single resonance conditions, the intensity of single resonance peaks is expected to be dominant in the Raman spectrum [38]. Double resonance can only be relevant for higher excitation energies. The condition set by Eq. 4 must also hold for SWNTs in order to have a significant EPC contribution to the linewidth. Eq. 4 can only be satisfied by phonons with wavevector too small to be double resonant [14, 15]. Thus, in double resonance, the G⁻ peak should be much narrower than experimentally observed. Interestingly, it has been reported that the broad G⁻ peak disappears by increasing the excitation energy while measuring the Raman spectrum of a metallic SWNT, and a sharper one appears [14]. We explain this as a transition from single to double resonance.

Finally, in Ref. [3] we computed the zero-temperature life-time τ of a conduction electron in a SWNT, due to phonon scattering. If phonons are thermalized, τ determines the electron mean free path $l_0 = \beta\tau/\hbar$ at zero temperature. The phonon linewidths can be expressed as a function of τ as:

$$\gamma_{\Gamma-LO}^{EP} = 4/\tau_{\Gamma-LO}^{bs} = 4/\tau_{\Gamma-TO}^{fs}, \quad (7)$$

where *bs*(*fs*) indicate back (forward)-scattering [3]. Such simple relations might seem surprising. In fact, the two quantities γ^{-1} and τ describe two distinct phenomena: γ^{-1} is the life-time of a phonon (Eq. 1) and τ is the life-time of an electron (Eq. 1 of Ref. [3]). In general, one does not expect a simple relation between γ^{-1} and τ . However, due to the low dimensionality, in SWNTs γ^{EP} determines directly τ (Eq. 7). Thus, the measured γ^{EP} are also a direct measurement of l_0 for metallic SWNTs. Since the measured γ^{EP} is in agreement with DFT calculations, the results of Ref. [3] are further confirmed.

In conclusion, we presented a set of simple formulas (Eqs. 2, 3, 6), with the graphite EPC as the *only* fit parameter. Remarkably, these formulas *quantitatively* explain a string of experiments, ranging from phonon slopes and FWHM(G) in graphite to G⁻ peak position

and FWHM(G⁻) diameter dependence in SWNTs. Fitting a wide set of independent data we obtain the *same* EPCs $\pm 10\%$. These experimental EPC are in excellent agreement with, and validate, the DFT approach.

Calculations performed at HPCF (Cambridge) and IDRIS (grant 051202). We acknowledge S. Reich and C. Thomsen for providing single crystal graphite; M. Oron and R. Krupke for useful discussions. Funding from EU IHP-HPMT-CT-2000-00209 and CANAPE, from EPSRC GR/S97613 and The Royal Society is acknowledged.

* Electronic address: lazzeri@impmc.jussieu.fr

† Electronic address: acf26@eng.cam.ac.uk

- [1] Z. Yao, C.L. Kane and C. Dekker, Phys. Rev. Lett. **84**, 2941 (2000).
- [2] J. Y. Park *et al.*, Nano Lett. **4**, 517 (2004).
- [3] M. Lazzeri *et al.* cond-mat/0503278.
- [4] V. Perebeinos, J. Tersoff, P. Avouris, Phys. Rev. Lett. **94**, 086802 (2005).
- [5] A. Javey *et al.*, Phys. Rev. Lett. **92**, 106804 (2004).
- [6] S. Piscanec *et al.* Phys. Rev. Lett. **93**, 185503 (2004).
- [7] M.A. Pimenta *et al.*, Phys. Rev. B **58**, 16016 (1998).
- [8] H. Kataura *et al.*, Synth. Metals **103**, 2555 (1999).
- [9] P. M. Rafailov, H. Jantoljak, and C. Thomsen, Phys. Rev. B **61**, 16179 (1999).
- [10] S.D.M. Brown *et al.*, Phys. Rev. B **63**, 155414 (2001).
- [11] A. Jorio *et al.*, Phys. Rev. B **65**, 155412 (2002); **66**, 115411 (2002); M. S. Dresselhaus *et al.*, Physica B **323**, 15 (2002).
- [12] C. Jiang *et al.*, Phys. Rev. B **66**, 161404 (2002).
- [13] K. Kempa, Phys. Rev. B **66**, 195406 (2002).
- [14] J. Maultzsch *et al.* Phys. Rev. Lett. **91**, 087402 (2003).
- [15] Jorio *et al.*; Thomsen *et al.*; Reich *et al.*; P. Tan *et al.* in *Raman spectroscopy in carbons: from nanotubes to diamond*, eds. A. C. Ferrari and J. Robertson Phil. Trans. Roy. Soc. A **362**, 2267-2565 (2004).
- [16] H. Telg *et al.*, *Proceedings of IWEPNM 2005* AIP, Melville, NY, 2005.
- [17] M. Oron, R. Krupke *et al.* Nano Lett. in press (2005).
- [18] S.K. Doorn *et al.*, Phys. Rev. Lett. **94**, 016802 (2005).
- [19] T. Hertel and G. Moos, Phys. Rev. Lett. **84**, 5002 (2000).
- [20] J. Jiang *et al.*, Chem. Phys. Lett. **392**, 383 (2004).
- [21] G.D. Mahan, Phys. Rev. B **68**, 125409 (2003).
- [22] G. Pennington and N. Goldsman, Phys. Rev. B **68**, 045426 (2004).
- [23] J. Jiang *et al.*, Phys. Rev. B **71**, 045417 (2005).
- [24] M. Paillet *et al.*, Phys. Rev. Lett. **64**, 327401 (2005).
- [25] S.M. Bose, S. Gayen, S.N. Behera, cond-mat/0506004.
- [26] P.B. Allen, Phys. Rev. B **6**, 2577 (1972); P.B. Allen and R. Silbergliitt, *ibid.* **9**, 4733 (1974).
- [27] J. Maultzsch *et al.* Phys. Rev. Lett. **92**, 075501 (2004).
- [28] F. Tuinstra, J. Koenig J. Chem. Phys. **53**, 1126 (1970).
- [29] The EPC dependence on **k** is given in Eq. 6 of Ref. [6]. A factor 2 in Eq. 3 accounts for both **K** and **K'**.
- [30] V. Scardaci, A. C. Ferrari, unpublished.
- [31] A.C. Ferrari and J. Robertson, Phys. Rev. B **61**, 14095 (2000); *ibid.* **64**, 075414 (2001).
- [32] P. Tan *et al.* Phys. Rev. B **64**, 214301 (2000).
- [33] S. Piscanec *et al.*, unpublished.

- [34] O. Dubay and G. Kresse, Phys. Rev. B **67**, 035401 (2003).
- [35] FWHM(G^-) and FWHM(G^+) increase $\sim 15 \text{ cm}^{-1}$ with temperature in the 80K-600K range for both metallic and semiconducting SWNTs [11, 30]. Thus $\gamma^{an} \ll \gamma^{EP}$.
- [36] J. Maultzsch, S. Reich, C. Thomsen, Phys. Rev. B **65** 233402 (2002)
- [37] C. Thomsen, S. Reich Phys. Rev. Lett. **85**, 5214 (2000).
- [38] M.A. Pimenta *et al.*, in *Proceedings of IWEPNM 2003* (AIP, Melville NY, 2003).